J. Biochem. 119, 42-48 (1996)

Analytical Studies of Spontaneous and Vasopressin-Induced Calcium Oscillations in Cultured Vascular Smooth Muscle Cells[1]

Sheng-Nan Wu,*,[2] Hsin-Su Yu,† and Yousuke Seyama‡

Department of Medical Education and Research, Kaohsiung-Veterans General Hospital, Kaohsiung, Taiwan; †Department of Dermatology, Kaohsiung Medical College, Kaohsiung, Taiwan; and ‡Department of Physiological Chemistry and Nutrition, Faculty of Medicine, The University of Tokyo, Bunkyo-ku, Tokyo 113

Received for publication, July 10, 1995

Spontaneous and vasopressin-induced Ca^{2+} oscillations in cultured vascular smooth muscle (A7r5) cells were further examined and characterized. Intracellular Ca^{2+} concentrations ($[Ca^{2+}]_i$) were measured by use of a high-performance laser cytometer. When the oscillatory patterns in $[Ca^{2+}]_i$ were analyzed with a power spectrum method, about 80% of cells exhibited spontaneous Ca^{2+} oscillations with the frequency of 0.02-0.5 Hz. Nifedipine abolished these repetitive spikes, whereas pinacidil partially attenuated their amplitude and frequency. When vasopressin (100 nM) was applied to A7r5 cells, there was an initial rise in $[Ca^{2+}]_i$, followed by a delayed sustained increase in $[Ca^{2+}]_i$. The one-pool, nonoscillatory model was employed to fit this biphasic change, and the difference between the observed response and the simulated response was then analyzed with a power spectral method. About 50% of cells were noted to display oscillatory patterns in $[Ca^{2+}]_i$ after sustained increase in $[Ca^{2+}]_i$. The present study indicates that spontaneous Ca^{2+} oscillations in A7r5 cells are modulated by the activity of ATP-sensitive K^+ channels and are not related to pertussis toxin-sensitive GTP-binding protein(s). On the basis of the one-pool, nonoscillatory model, it is suggested that the buffering capacity of internal stores appears to be stronger in the cells with spontaneous Ca^{2+} oscillations than in those in a quiescent state, and the vasopressin-mediated inhibition of accumulation by internal stores was attenuated when the cells exhibited spontaneous Ca^{2+} oscillations. The implementation of this minimum kinetic model integrated with a power spectrum method would be an alternative to understand the oscillating behavior in $[Ca^{2+}]_i$.

Key words: Ca^{2+} oscillations, power spectrum, smooth muscle cell, vasopressin.

The alteration of cytosolic Ca^{2+} ($[Ca^{2+}]_i$) is essentially related to smooth muscle contraction (*1*), whereas tension oscillations in vascular smooth muscle are mediated *via* cytosolic Ca^{2+} oscillations existing in vascular smooth muscle cells (*2*). Cultured vascular smooth muscle (A7r5) cells have been reported to undergo spontaneous Ca^{2+} oscillations, which required good structural and electrical contact among cells (*3, 4*). Although this type of Ca^{2+} oscillations was thought to be attributable to intrinsic activity derived from the surface membrane, little is known about whether the concentration of intracellular ATP contributes to the occurrence of spontaneous Ca^{2+} oscillation, or whether the activity of ATP-sensitive K^+ channels (*5*) is required for the maintenance of spontaneous Ca^{2+} oscillations.

Cytosolic Ca^{2+} oscillations have been qualitatively modelled in an attempt to understand their underlying mechanisms (*6*). However, in a variety of cell types, the oscillatory pattern in the agonist-evoked Ca^{2+} spikes appeared to show rather wide variation that most mathematical models presented in the form of a pure sinusoid pattern cannot readily represent. Besides, only a single population of intracellular stores could clearly be demonstrated in A7r5 cells (*3*), while most theoretical models for this oscillatory phenomenon were designed on the basis of either a two-pool version (*6-9*) or the periodic increase in the level of intracellular inositol trisphosphate (IP_3) (*10*). Even though these models may in part qualitatively fit the experimental data, their explanation of the geneses of Ca^{2+} oscillation is not realistic (*9*). Recently, Dupont and Goldbeter (*11*) proposed a one-pool model for Ca^{2+} oscillations involving Ca^{2+} and IP_3 as co-agonists for Ca^{2+} release from internal stores. However, in our view, this model is still unsatisfactory, because the simulation result showing that the first Ca^{2+} spike is always larger than the following ones appeared not to be in agreement with some experimental data, at least in our preparations. For instance, agonists produced an initial large peak in $[Ca^{2+}]_i$ and an ensuing sustained increase in $[Ca^{2+}]_i$. Immediately after the sustained increase in $[Ca^{2+}]_i$, a train of Ca^{2+} spikes was noted (*12, 13*). To clearly understand this diverse pattern of Ca^{2+} oscillations, a better mathematical model needs to be designed and analyzed. Therefore, in the present study, we chose the one-pool, nonoscillatory model originally described by Rønes and Røttingen (*14*) and examined its fit

[1] This study was supported in part by grants from Kaohsiung-Veterans General Hospital (VGHKS-85-60) and National Science Council (NSC-85-2331-B-075B-012), Taiwan.

[2] To whom correspondence should be addressed. Tel: 886-7-3422121-1507, Fax: 886-7-3468056, E-mail: shenga@cc.nsysu.edu.tw

to the vasopressin-induced biphasic change in $[Ca^{2+}]_i$. Subsequently, a power spectrum method was analyzed between the observed and simulated response in order to quantitatively understand the behavior of Ca^{2+} oscillations in A7r5 cells.

MATERIALS AND METHODS

Materials—Molecular Probes (Eugene, OR) supplied indo-1 acetoxymethyl ester (AM) and pluronic F-127. Arginine^8-vasopressin (vasopressin) and endothelin-1 were obtained from Peptide Institute (Osaka). Ionomycin, nifedipine, EGTA [ethylglycol-bis-(β-aminoethyl)-*N,N,N′,N′*-tetraacetic acid], HEPES (*N*-2-hydroxyethylpiperazine-*N′*-2-ethanesulphonic acid), and ATP (5′-adenosine triphosphate) were all purchased from Sigma Chemical (St. Louis, MO). Pinacidil was from Leo Pharmaceuticals (Denmark). Nicorandil was from Chugai Pharmaceuticals (Tokyo). Pertussis toxin was from List Biological Laboratories (Campbell, CA). Tissue culture media, penicillin-streptomycin, and trypsin were from Gibco (Grand Island, NY). All other chemicals were obtained from regular commercial sources and were of reagent grade.

Cell Culture—Rat thoracic aorta smooth muscle cells (clonal cell line A7r5, originally obtained from American Type Culture Collection, [CRL1444], Rockville, MD) were maintained and subcultured in Dulbecco's modified Eagle's medium (DMEM) supplemented with fetal bovine serum (10%), penicillin G (10,000 units/ml), and streptomycin (10 mg/ml), and equilibrated at 37°C with a humidified atmosphere of 95% air/5% CO_2 air. Cells were subcultured weekly after detachment by using culture medium containing 1% trypsin. The experiments were performed after cells reached confluence (usually 5–7 days). In some experiments, cells were incubated with pertussis toxin (500 ng/ml) at 37°C for 24 h.

Cytosolic Free Ca^{2+} Concentration Measurements—Monolayer cultures of A7r5 vascular smooth muscle cells were grown in an experimental chamber which consisted of a modified 35 mm plastic Petri dish, with an 18 mm diameter hole in the center. A glass coverslip was glued over the hole so as to allow visual observation, dye excitation and detection of dual emission in an inverted microscopy with a D Apo 100X UV oil immersion objective (numerical aperture, 1.3) (IMT-2, Olympus, Tokyo) connected with the fluorometer.

On the day of experiment, the culture medium in the Petri dish was replaced with a "loading solution" containing 3 μM indo-1 acetoxymethyl ester (indo-1/AM) and 3 μM pluronic F-127. The dish was incubated for 60 min, then washed three times with normal Tyrode solution containing (in mM): NaCl, 136.5; KCl, 5.4; $CaCl_2$, 1.8; $MgCl_2$, 0.53; glucose, 5.5; HEPES, 5; and NaOH to adjust pH to 7.4.

The dynamic change in cytosolic free Ca^{2+} concentrations ($[Ca^{2+}]_i$) was measured at room temperature using the ratiometric approach with the fluorescent, calcium indicator indo-1/AM (*15–17*). The control of the microscope stage position, excitation of the calcium probe, and recording of dual emission were performed by an interactive laser cytometer ACAS 570 (Meridian Instruments, Okemos, MI). In the present experiments, the laser intensity was set to 10–20% of the 20 mW output and a neutral density filter which only passes 10% of the light was also used. The excitation laser beam (about 0.6 μm in diameter) was directed to the specimen through the epi-illumination port of the microscope and a cube containing an excitation filter (350 nm, band pass) and a dichroic mirror (380 nm). The dual emission of the excited probe was collected through this dichroic mirror and a barrier filter (390 nm, long pass) and two band pass filters (485/45 nm and 405/45 nm). This allowed the detection of fluorescence emissions of both free and Ca^{2+}-bound forms of the dye by two separate photomultiplier tubes. The other important parameters, including sampling frequency (100, 20, or 5 Hz in the present experiments), illumination intensity, detector gains, and the number of measurements (generally 256) averaged for each set of sampled data were adjusted by means of the control software of the Northgate computer (Minneapolis, MN). The initial fluorescent intensities were always adjusted to be near mid-range on the fluorescent scale to obtain sufficient dynamic range. To obtain the highest time resolution, Ca^{2+} measurements were made in the "point scan" mode; that is, a single point within the cell is continuously monitored in milliseconds.

Calculation of Intracellular Ca^{2+} Concentrations—The *in vivo* calibration of indo-1 fluorescence was performed by use of the established protocols (*17*). Briefly, the baseline fluorescence was recorded from indo-1-loaded cells in control solution. The cells were then permeabilized by exposure to 10 μM ionomycin under depolarizing conditions at pH 8.6. Cells were then exposed in a bathing solution containing 10 mM Ca^{2+}, and R_{max} (fluorescence ratio for the bound dye) was measured as the peak ratio during this preparation. The bathing solution was replaced with one containing 10 mM EGTA and no added Ca^{2+} (0 Ca^{2+} bathing solution), and R_{min} (the fluorescence ratio for the unbound dye) was determined as the ratio minimum. Finally, the autofluorescence was determined by exposing cells to 20 mM Mn^{2+} and 10 μM ionomycin. $[Ca^{2+}]_i$ values were calculated from measured indo-1 fluorescence ratios with the following formula

$$[Ca^{2+}]_i = K_d \times \left(\frac{S_{f2}}{S_{b2}}\right) \times \left[\frac{R - R_{min}}{R_{max} - R}\right]$$

where K_d is the apparent dissociation constant of the Ca^{2+}/indo-1 complex and is taken as 250 nM (*15*). S_{f2}/S_{b2} is the ratio of the 485 nm fluorescence obtained with the Ca^{2+}-free and Ca^{2+}-bound forms of the dye. Although the values observed in the resting $[Ca^{2+}]_i$ were within the acceptable range for living cells, the measurements required care because of the great variability in indo-1 fluorescence (*18*).

Power Spectral Analysis and Computer Simulations—The frequency and amplitude of cytosolic Ca^{2+} oscillations were characterized by transforming the oscillating signals from their time domain to their representation in the frequency domain with the aid of power spectrum analysis. Spectral analysis was done using a discrete Fourier transform algorithm (*19*). The main spectral component was taken as the frequency which showed greatest amplitude in the power spectrum. In other words, an oscillating signal throughout the observation interval would be presented as one outstanding spike at the corresponding frequency with a positive correlation between the height of the spike and the amplitude of the oscillating signal. Accordingly, a measure of the tendency of the cells to oscillate in $[Ca^{2+}]_i$ was defined by the height of the spike with its correspond-

ing frequency.

The vasopressin-induced biphasic change in $[Ca^{2+}]_i$ was simulated by use of the one-pool, nonoscillatory model originally designed by Røtnes and Røttingen (*14*). This nonlinear mathematical model, which is defined by five adjustable parameters, is a relatively simple scheme and was thought to be capable of fitting our experimental results with A7r5 cells (*20*). Therefore, the simulations shown herein were generated according to the model of Røtnes and Røttingen (*14*), using similar numerical parameters.

The equations for a one-pool, nonoscillatory model (*14*) are:

$$\frac{dZ}{dt} = v_{qr} \times \sqrt{Z} + k_f \times Y - k \times Z$$

$$\frac{dY}{dt} = -v_{qr} \times \sqrt{Z} - k_f \times Y + k \times Z$$

$$v_{qr} = V_{QR} \times \frac{1}{1+\left(\frac{K_R}{Y}\right)^2} \times \frac{1}{1+\left(\frac{K_I}{[IP_3]}\right)^2}$$

$$[IP_3] = ((1-\alpha)e^{\frac{-(t-t_0)}{\tau_I}} + \alpha) \times u(t-t_0)$$

$$Z(t_0) = \text{mean observed } [Ca^{2+}]_i \ (t < t_0)$$

$$k = k_f \times \frac{Y(t_0)}{Z(t_0)}$$

where Y and Z are the Ca^{2+} in internal stores and cytosolic Ca^{2+}, respectively; k_f and k denote the rate constants of Ca^{2+} ions out of and into the internal stores, respectively; v_{qr} refers to the quantal release of Ca^{2+} from internal stores, which is elicited by Ca^{2+} ions and IP_3; K_R and K_I are the threshold constants for Ca^{2+} release induced by Ca^{2+} ions and IP_3, respectively; τ_I denotes the time constant for IP_3 production; α is the steady-state value; and $u(t)$ is a unit step function. Based on this model, there are five parameters that are adjustable, *i.e.*, $Y(t_0)$, V_{QR}, k_f, τ_I, α, and t_0.

When a strong correlation was found between the observed and the simulated responses, the difference between them was taken and a power spectrum method was then implemented to analyze the fundamental frequency of Ca^{2+} oscillations.

Data Recording and Analyses—The image data were captured with a Northgate computer using the PEPPER SGT Plus board (Number Nine Computer, Cambridge, MA), which was built into the Meridian integrated system. The digital data were stored into an optical disk and subsequently analyzed by use of the Meridian DASY 9000 workstation. Hard-copy graphic printouts were obtained using a Hewlett-Packard Paintjet printer (San Diego, CA).

The data were analyzed by standard statistical techniques, including the calculation of mean values, standard error of the mean (SEM), paired or unpaired t test, linear regression and correlation coefficient. The level of significance was taken at $p<0.05$. All analyses were performed by a general-purpose personal computer equipped with an Intel 80486 microprocessor.

RESULTS

As illustrated in panel A of Fig. 1, a typical pattern of spontaneously sinusoid Ca^{2+} oscillations was observed in an indol-loaded A7r5 cell. When the signals shown in panel A were transformed from their time domain to their representation in the frequency domain with the aid of power spectrum analysis, a large peak became apparent in the power spectrum with a corresponding frequency of 0.35 Hz (panel B of Fig. 1). When the power spectrum analysis was applied, about 80% of cells were noted to display spontaneous Ca^{2+} oscillations, the frequency of which is rather variable, ranging between 0.02 and 0.5 Hz. However, once normal Tyrode's solution was replaced with Ca^{2+}-free solution containing 10 mM EGTA, spontaneous Ca^{2+} oscillations failed to be detected. Furthermore, during the spontaneous and regular Ca^{2+} oscillations, the addition of nifedipine (3 μM) remarkably suppressed the amplitude and frequency of the spiking pattern (Fig. 2), and 2-3 min later, the rhythmical activity was completely abolished. However, caffeine (10 mM) failed to abolish this spontaneous rhythmical activity. These findings indicated that spontaneous Ca^{2+} oscillations present in A7r5 cells were dependent on extracellular Ca^{2+} concentration and related to the activity of the L-type voltage-dependent Ca^{2+} channel (*3*).

To understand whether the ATP-dependent K^+ channel is involved in the activity of spontaneous Ca^{2+} oscillations, the effect of pinacidil, an opener of the ATP-activated K^+ channel, was also examined. As shown in Fig. 3, when the A7r5 cells were constantly exposed to pinacidil (100 μM), the frequency and amplitude of spontaneous Ca^{2+} spiking was slightly reduced, and 5-10 min after the addition, the quasi-regular Ca^{2+} oscillations were still observed. Similar results were obtained in five different cells. The application of nicorandil (100 μM) produced similar results. These

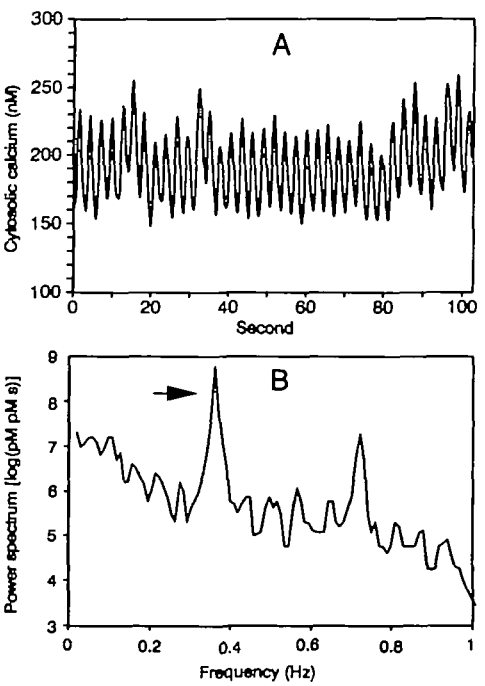

Fig. 1. **Spontaneous Ca^{2+} oscillations in an A7r5 cell.** Panel A is the repetitive change in Ca^{2+} transients and panel B shows the frequency domain to which spectral analysis function transformed time-domain signals derived from panel A. The arrow indicates a large peak which corresponds to the frequency of Ca^{2+} oscillations.

effects appeared to be relatively less than that caused by nifedipine. Moreover, spontaneous repetitive Ca^{2+} spikes can still be observed in pertussis toxin-pretreated cells, which indicates that spontaneous Ca^{2+} oscillations in A7r5 cells do not involve the activity of pertussis toxin-sensitive protein(s).

Vasopressin-induced change in $[Ca^{2+}]_i$ in A7r5 cells was also studied. During the time that the Ca^{2+} transients were not oscillatory, the addition of vasopressin (100 nM) produced an initial rapid rise in $[Ca^{2+}]_i$, followed by a delayed and sustained increase in $[Ca^{2+}]_i$. However, immediately after the vasopressin-induced biphasic change in $[Ca^{2+}]_i$, a train of repetitive, quasi-regular Ca^{2+} spikes was always observed. One example is illustrated in panel A of Fig. 4. Similar results were also observed in the application of endothelin-1 (100 nM) on $[Ca^{2+}]_i$. In addition, neither nifedipine nor pinacidil caused any significant change in vasopressin-induced Ca^{2+} oscillations (data not shown). These findings indicate that the mechanism of vasopressin-induced Ca^{2+} oscillations is different. To analyze quantitatively this unique pattern of vasopressin-induced Ca^{2+} oscillations, the one-pool, nonoscillatory model originally designed by Røtnes and Røttingen (*14*) was used to fit our experimental results. As shown in panel A of Fig. 4, the smooth line denotes a convincing fit to the real event when the numerical parameters were appropriately chosen. The observed and the simulated values were found to correlate in a linear manner (panel B of Fig. 4). Panel C of Fig. 4 shows the power spectrum calculated from the difference between these two responses. Of particular interest is the evidence that the fundamental frequency reflected by the

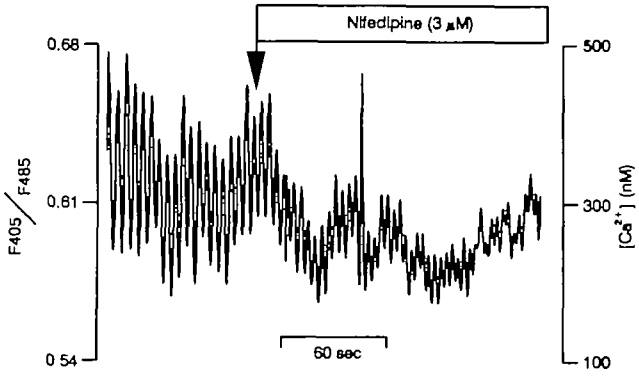

Fig. 2. **Effect of nifedipine on spontaneous Ca^{2+} oscillations in an A7r5 cell.** The addition of nifedipine (10 μM) suppressed the amplitude and frequency of Ca^{2+} oscillations.

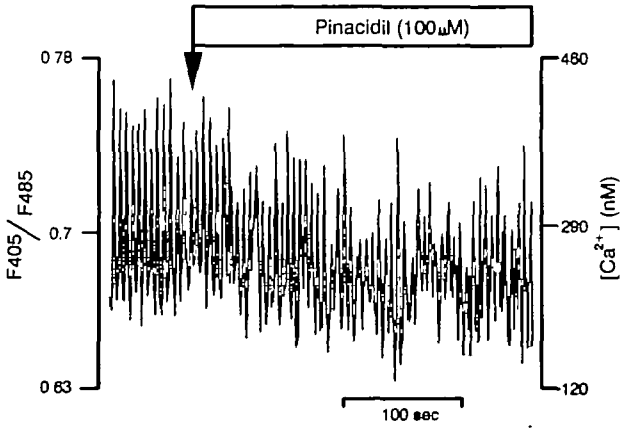

Fig. 3. **Effect of pinacidil on spontaneous Ca^{2+} oscillations in an A7r5 cells.** The application of pinacidil (100 μM) partially attenuated the amplitude and frequency of Ca^{2+} oscillations.

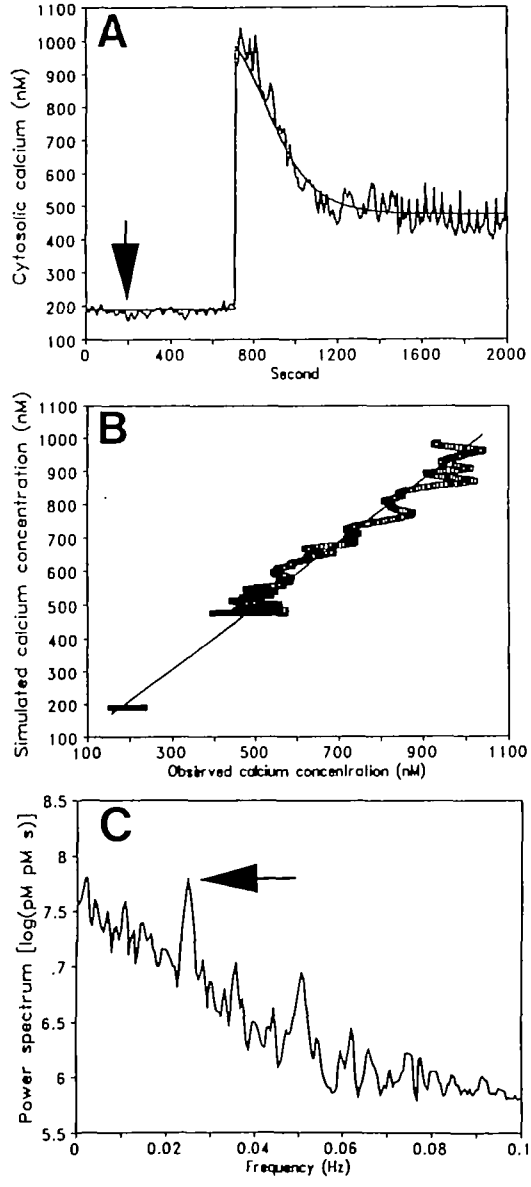

Fig. 4. **Analyses of vasopressin-induced Ca^{2+} oscillations in an A7r5 cell.** Panel A is the time course of vasopressin effect on Ca^{2+} transients. The addition of vasopressin caused a large rise in $[Ca^{2+}]_i$ and a delayed and sustained increase in $[Ca^{2+}]_i$. Of note, immediately after the sustained elevation in $[Ca^{2+}]_i$, a train of Ca^{2+} spikes with smaller magnitude developed. The smooth line indicates the best-fit curve with $Y(t_0)=1{,}100$ nM, $V_{OR}=100\ s^{-1}$, $\tau_1=130$ s, $t_0=689$ s, $\alpha=0.23$ and $k_f=0.020\ s^{-1}$. A detailed explanation of the one-pool, nonoscillatory model is given in "MATERIALS AND METHODS" and Ref. *14*. Panel B shows the linear relationship of observed values *versus* simulated values with $r=0.99$ and slope $=1$. Panel C illustrates the result of power spectral analysis which was done when the difference of simulated values and observed values were taken. The arrow indicates a large peak which corresponds to the frequency of Ca^{2+} oscillations.

outstanding peak turned out to be 0.025 Hz. Similar experiments were done with 12 different cells. If the analytical studies were not performed, only about 10% of cells were found to develop Ca^{2+} oscillations following the sustained increase in $[Ca^{2+}]_i$. However, with the aid of this kind of analytical method, vasopressin-induced Ca^{2+} oscillations could be either predicted or found in up to 50% of cells.

Likewise, when A7r5 cells which displayed Ca^{2+} oscillations were exposed to vasopressin (100 nM), a large rise and the ensuing sustained increase in $[Ca^{2+}]_i$ were also observed. The oscillatory pattern became small and irregular immediately after the biphasic change in $[Ca^{2+}]_i$ caused by vasopressin (panel A of Fig. 5). To further characterize this biphasic change in $[Ca^{2+}]_i$ and Ca^{2+} oscillations, the one-pool, nonoscillatory model was again implemented to fit these experimental data. The simulated line shown in panel A of Fig. 5 revealed a linear correlation between the observed and the simulated values (panel B of Fig. 5). Panels C and D of Fig. 5, respectively, demonstrate the power spectra in which the main spectral component, taken as the frequency with the greatest amplitude, was 0.036 and 0.009 Hz, respectively. In other words, after the vasopressin-induced biphasic change in $[Ca^{2+}]_i$, the frequency of Ca^{2+} oscillations was reduced from 0.036 Hz (panel C) to 0.009 Hz (panel D). When a higher concentration of vasopressin (1 μM) was applied, the biphasic change was still observed but the Ca^{2+} spikes became silent.

Table I summarizes the difference in these parameter values obtained from the simulated response of A7r5 cells to vasopressin (100 nM) between the absence and presence of spontaneous Ca^{2+} oscillations. Interestingly, the simulated value of $Y(t_0)$, which refer to the basal Ca^{2+} concentrations inside the internal stores, was significantly larger in cells with spontaneous Ca^{2+} oscillations, whereas measured basal $[Ca^{2+}]_i$ did not significantly differ between Ca^{2+}-oscillating and nonoscillating cells, *i.e.*, 210 ± 10 *versus* 202 ± 9 nM ($n=7$). Conversely, the rate constant for

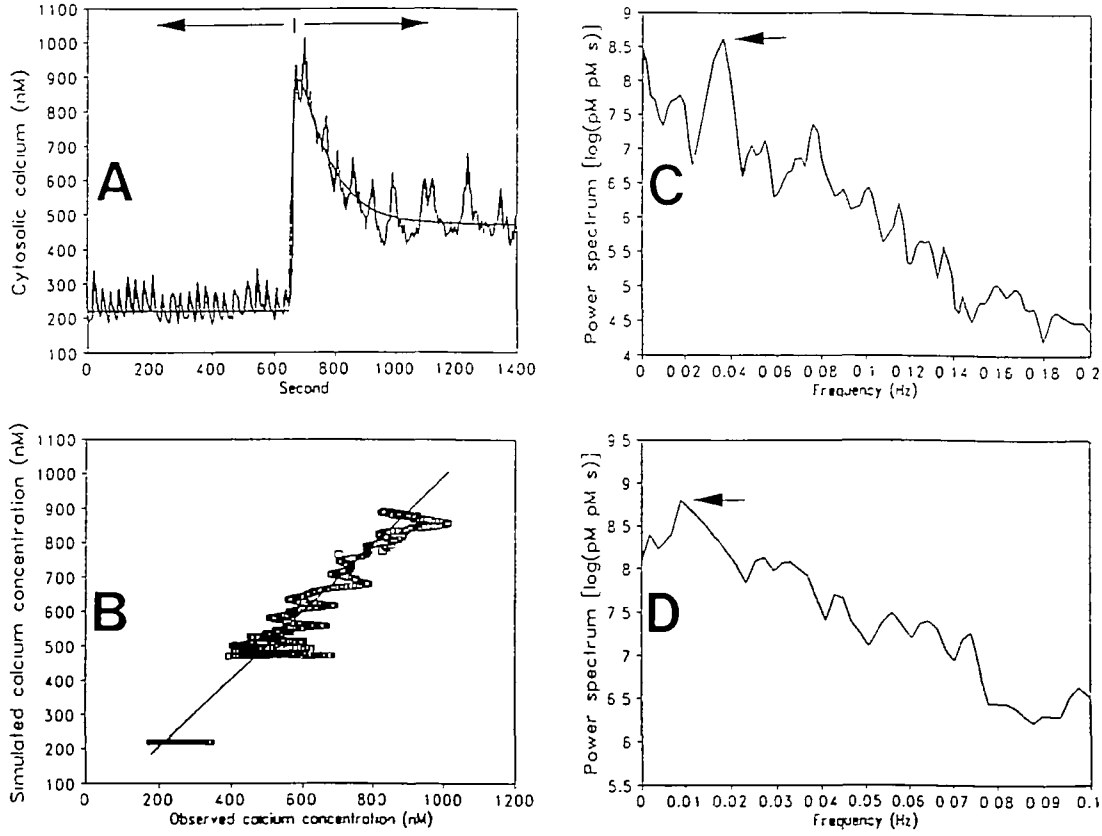

Fig. 5. **Analyses of Ca^{2+} oscillations superimposed upon the biphasic changes in $[Ca^{2+}]_i$ induced by the addition of vasopressin.** As illustrated in panel A, when spontaneous, regular Ca^{2+} oscillations existed, further application of vasopressin (100 nM) caused a biphasic change in Ca^{2+} transients and a train of Ca^{2+} spikes with quasi-regular frequency was noted. The corresponding parameters derived from the one-pool, nonoscillatory model were then employed to fit the nonlinear, biphasic change in $[Ca^{2+}]_i$. The smooth line indicates the best-fit curve. The corresponding parameters are as follows: $Y(t_0)=2{,}800$ nM, $V_{OR}=38\ s^{-1}$, $\tau_1=120$ s, $t_0=660$ s, $\alpha=0.45$ and $k_f=0.020\ s^{-1}$. A detailed explanation of the one-pool, nonoscillatory model is given in "MATERIALS AND METHODS" and Ref. *14*. The arrows shown in panel A indicate that the power spectrum analysis was divided to two periods, *i.e.*, before and after the biphasic change. The validity of good correlation between the observed values and the simulated values was shown in panel B with $r=0.99$ and slope $=1.0$. Subsequently, the difference between the observed values and the simulated values was taken and the power spectral method was then employed. Panel C indicates the result derived from the digital values prior to the development of a large peak in Ca^{2+} transients, whereas panel D is the result showing the frequency domain immediately after the initial rise in Ca^{2+} transients. The arrows in panels C and D denote the outstanding peaks which correspond to the frequency of Ca^{2+} oscillations. Of note, the large peak representing the outstanding frequency domain analyzed from the occurrence prior to the biphasic change is different from that after biphasic change.

TABLE I. **The parameter values obtained from the simulated responses of A7r5 cells to vasopressin with the one-pool, nonoscillatory model.** Values are mean±SEM. These parameters are explained in detail in "MATERIALS AND METHODS." NS, not significant.

	A7r5 cells without spontaneous Ca^{2+} oscillations ($n=7$)	A7r5 cells with spontaneous Ca^{2+} oscillations ($n=5$)	p
$Y(t_0)$ (nM)	1080±140	2750±150	0.05
V_{QR} (1/s)	102±10	39±5	0.05
τ_1 (s)	130±7	124±8	NS
α	0.23±0.08	0.44±0.08	0.05
k_f (1/s)	0.021±0.008	0.020±0.007	NS

maximal quantal release of Ca^{2+} from the internal store is greater in nonoscillating cells. However, there are no significant differences in τ_1 and k_f between oscillating and nonoscillating cells.

DISCUSSION

The present studies support the evidence that spontaneous Ca^{2+} oscillations in A7r5 cells are derived from the pacemaker activity of the surface membrane (*3*). However, the finding that caffeine does not suppress these oscillations is against the notion that it is related to the release of Ca^{2+} from internal stores (*21*). This Ca^{2+} spike was abolished by the blocker of L-type voltage-dependent Ca^{2+} channel, nifedipine, and was attenuated by the opener of ATP-dependent K^+ channel, pinacidil. The later finding suggests that (i) mild membrane hyperpolarization caused by pinacidil will affect spontaneous Ca^{2+} oscillations, and (ii) the basal concentration of ATP inside the cells could be sufficient to keep ATP-sensitive K^+ channels closed even though pinacidil (100 μM) was present. Thus, under appropriate conditions, the ATP-dependent K^+ channel may play an essential role in the regulation of pacemaker activity in A7r5 cells as described in the other types of cells (*5, 22*).

A previous report showed that the pacemaker activity of locus coeruleus neuron could be activated *via* the cyclic AMP-dependent protein phosphorylation pathway (*23*). Therefore, when the cells were pretreated with pertussis toxin, which ADP-ribosylates α-subunits of inhibitory GTP-binding protein(s), the Ca^{2+} oscillations related to the pacemaker activity in surface membrane could be increased. However, this was not the case. In pertussis toxin-treated A7r5 cells, the spontaneous Ca^{2+} oscillations were still observed and their amplitude and frequency remained unaltered, which indicates that pertussis toxin-sensitive GTP-binding protein(s) are not related to the basal pacemaker activity in A7r5 cells. However, it is also hard to exclude the possibility that A7r5 cells may lack α subunits of inhibitory GTP-binding protein(s).

The method for calculating the power spectrum is not unique. A variety of techniques are available for power spectral analysis (*19*). The power spectrum method adopted in the present study is a conventional technique based on the fast Fourier transform, because the simplest fast Fourier method could be applicable to determine the fundamental frequency as the frequency which has the greatest amplitude within the spectrum. In fact, the efficiency of this analytical procedure shown in the present study was validated by the analyses of various sinusoid signals. Nevertheless, the selection of any power spectrum method is considerably aided by the availability of a model of the mechanisms that generate the phenomenon. In the present study, with the aid of the power spectral analysis which converts the time domain to the frequency domain, the fraction of the population of A7r5 cells which exhibits or tends to have spontaneous Ca^{2+} oscillations was noted to be increased. Its frequency appeared to be regular with the range of 0.02–0.5 Hz. The reason for the variable oscillating frequency of Ca^{2+} transients in our preparations could be a dependence on electrical and/or structural coupling among cells (*4*). In addition, because Ca^{2+} oscillation was noted to be encoded through a frequency-dependent cellular response, such as protein phosphorylation and dephosphorylation (*7*), the implementation of the power spectral method to determine the pattern of frequency domain would be useful to study the extent to which this kind of encoding process is linked.

There are three reasons why part of the observations of vasopressin-induced biphasic change in $[Ca^{2+}]_i$ could be defined within the framework of this one-pool, nonoscillatory model. First, the latency for the development of vasopressin-induced biphasic response is not constant. However, one of numerical parameters, *i.e.*, $t(0)$, could be chosen to simulate this time difference. More interestingly, this different latency for the vasopressin response in individual cells existing in the same dish is suggested to be involved in the electrical coupling among the cells (*4*). Second, the initial rise in $[Ca^{2+}]_i$ produced by vasopressin is also dose-dependent. As long as the parameters were suitably adjusted, the diverse biphasic change arising from different concentrations of vasopressin could also be simulated (*14*). Third, because cellular and subcellular heterogeneity of $[Ca^{2+}]_i$ were present (*13, 24–26*) and vasopressin-induced Ca^{2+} oscillations appeared to be irregular and not constant, it is not easy to detect or predict the oscillating change in $[Ca^{2+}]_i$. Once the biphasic change was simulated and removed, the implementation of power spectral analysis would become a good approach to predict many aspects of the behavior of repetitive Ca^{2+} spikes. Interestingly, since electrically coupled cells are noted to be related to spontaneous Ca^{2+} oscillations (*4*), whether the power spectral analysis for each cell might be useful to understand the function of the tight junction is worthy of further examination.

A recent report shows that internal stores, particularly beneath the surface membrane, serve as a physiologically regulated barrier to Ca^{2+} diffusion into the cell interior (*25*). However, it is not easy to directly and precisely measure the Ca^{2+} concentrations inside the internal stores. By comparison with the present results derived from panels A of Figs. 4 and 5, the simulated basal Ca^{2+} concentration in internal stores ($Y(t_0)$) appeared to be larger in spontaneously Ca^{2+}-oscillating A7r5 cells than in cells without the presence of Ca^{2+} spikes (Table I), although the basal $[Ca^{2+}]_i$ in the two groups of cells was not significantly different. However, the cells with the spontaneous Ca^{2+} oscillations have less capacity to cause IP_3-activated Ca^{2+} release (V_{QR}) than the quiescent cells (Table I). Therefore, these results extend the implication that when the pacemaker activity is present, the refilling of the internal stores of Ca^{2+} is facilitated by the periodic change in membrane potential (*27*). Furthermore, it is likely that the existence

of spontaneous Ca^{2+} oscillations prevents the IP_3-induced inhibition of Ca^{2+} accumulation by internal stores and any alteration in pacemaker activity leads to affect the buffering capacity of internal stores (*17, 28*).

Although GTP-binding protein(s) are essentially components of the transduction mechanisms whereby the vasopressin action occurs, the present model used for the quantitative measurement of Ca^{2+} oscillations did not take these proteins into account for the sake of simplicity. However, the concept of the quantal release of Ca^{2+} ions from internal stores (*29*) was introduced to this model; hence the proposal for periodic release of IP_3 caused by agonists (*10*) would not necessarily be allowed to be included. In fact, agonist-induced Ca^{2+} oscillations should not require the periodic change in intracellular IP_3 (*30*).

In summary, the present studies provide the experimental and analytical methods to understand the spontaneous Ca^{2+} oscillations and vasopressin-induced biphasic changes in Ca^{2+} transients and the ensuing repetitive Ca^{2+} oscillations in A7r5 cells. This new approach in quantitative measurements of the oscillating behavior in $[Ca^{2+}]_i$ shown in the present experiments should be of great help in the study of the underlying mechanisms of rhythmic behaviors inside cells.

REFERENCES

1. Somolyo, A.P. and Himpens, B. (1989) Cell calcium and its regulation in smooth muscle. *FASEB J.* **3**, 2266-2276
2. van Breemen, C. and Saida, K. (1989) Cellular mechanisms regulating $[Ca^{2+}]_i$ in smooth muscle. *Annu. Rev. Physiol.* **51**, 315-329
3. Byron, K.L. and Taylor, C.W. (1993) Spontaneous Ca^{2+} spiking in a vascular smooth muscle cell line is independent of the release of intracellular Ca^{2+} stores. *J. Biol. Chem.* **268**, 6945-6952
4. Missiaen, L., Oike, M., Bootman, M.D., De Smedt, H., Parys, J., and Casteels, R. (1994) Vasopressin responses in electrically coupled A7r5 cells. *Pflügers Arch.* **428**, 283-287
5. Bolton, T.B. and Zhang, H. (1995) Activation by intracellular GDP, metabolic inhibition and pinacidil of a glibenclamide-sensitive K-channel in smooth muscle cells of rat mesenteric artery. *Br. J. Pharmacol.* **114**, 662-672
6. Berridge, M.J. (1991) Cytoplasmic calcium oscillations: A two pool model. *Cell Calcium* **12**, 63-72
7. Goldbeter, A., Dupont, G., and Berridge, M.J. (1990) Minimal model for signal-induced Ca^{2+} oscillations and for their frequency encoding through protein phosphorylation. *Proc. Natl. Acad. Sci. USA* **87**, 1461-1465
8. Kuba, K. and Takeshita, S. (1981) Simulation of intracellular Ca^{2+} oscillation in a sympathetic neurone. *J. Theor. Biol.* **93**, 1009-1031
9. Payet, M.D., Bilodeau, L., Héroux, J., Harbec, G., and Dupuis, G. (1991) Spectrofluorimetric and image recordings of spontaneous and lectin-induced cytosolic calcium oscillations in Jurkat T cells. *Cell Calcium* **12**, 325-334
10. Cuthbertson, K.S.R. and Chay, T.R. (1991) Modelling receptor-controlled intracellular calcium oscillators. *Cell Calcium* **12**, 97-109
11. Dupont, G. and Goldbeter, A. (1993) One-pool model for Ca^{2+} oscillations involving Ca^{2+} and inositol-trisphosphate as co-agonists for Ca^{2+} release. *Cell Calcium* **14**, 311-322
12. Woods, N.M., Cuthbertson, K.S.R., and Cobbold, P.H. (1987) Agonist-induced oscillations in cytoplasmic free calcium in single rat hepatocytes. *Cell Calcium* **8**, 79-100
13. Johnson, E.M., Theler, J.M., Capponi, A.M., and Vallotton, M.B. (1991) Characterization of oscillations in cytosolic free Ca^{2+} concentration and measurement of cytosolic Na^+ concentration changes evoked by angiotensin II and vasopressin in individual rat aortic smooth muscle cells. Use of microfluorometry and digital imaging. *J. Biol. Chem.* **266**, 12618-12626
14. Røtnes, J.S. and Røttingen, J.-A. (1994) Quantitative analysis of cytosolic free calcium oscillations in neutrophils by mathematical modelling. *Cell Calcium* **15**, 467-482
15. Grynkiewicz, G., Poenie, M., and Tsien, R.Y. (1985) A new generation of Ca^{2+} indicators with greatly improved fluorescence properties. *J. Biol. Chem.* **260**, 3440-3450
16. Wahl, M., Lucherini, M.J., and Gruenstein, E. (1990) Intracellular Ca^{2+} measurement with indo-1 in substrate-attached cells: Advantages and special considerations. *Cell Calcium* **11**, 487-500
17. Wu, S.N., Yu, H.S., and Seyama, Y. (1995) Induction of Ca^{2+} oscillations by vasopressin in the presence of tetraethylammonium chloride in cultured vascular smooth muscle cells. *J. Biochem.* **117**, 309-314
18. Owen, C.S., Sykes, N.L., Shuler, R.L., and Ost, D. (1991) Non-calcium environmental sensitivity of intracellular indo-1. *Anal. Biochem.* **192**, 142-148
19. Kay, S.M. and Marple, S.L., Jr. (1981) Spectrum analysis. A modern perspective. *Proc. IEEE* **69**, 1380-1419
20. Brown, D. and Rothery, P. (1993) Advanced model fitting in *Models in Biology*, pp. 423-457, John Wiley & Sons, West Sussex
21. Weissberg, P.L., Little, P.J., and Bobik, A. (1989) Spontaneous oscillations in cytoplasmic calcium concentration in vascular smooth muscle. *Am. J. Physiol.* **256**, C951-C957
22. Corkey, B.E., Tornheim, K., Deeney, J.T., Glennon, M.C., Parker, J.C., Matschinsky, F.M., Ruderman, N.B., and Prentki, M. (1988) Linked oscillations of free Ca^{2+} and the ATP/ADP ratio in permeabilized RINm5F insulinoma cells supplemented with a glycolyzing cell-free muscle extract. *J. Biol. Chem.* **263**, 4254-4258
23. Alreja, M. and Aghajanian, G.K. (1991) Activation of locus coeruleus neurons by cholera toxin: Mediation by cAMP-dependent protein kinase. *Neurosci. Lett.* **134**, 113-117
24. Goldman, W.F. (1991) Spatial and temporal resolution of serotonin-induced changes in intracellular calcium in a cultured arterial smooth muscle cell line. *Blood Vessels* **28**, 252-261
25. van Breemen, C., Chen, Q., and Laher, I. (1995) Superficial buffer barrier function of smooth muscle sarcoplasmic reticulum. *Trends Pharmacol. Sci.* **16**, 98-105
26. Kuba, K.K., Nohmi, M., and Hua, S.-Y. (1991) Intracellular Ca^{2+} dynamics in response to Ca^{2+} influx and Ca^{2+} release in autonomic neurones. *Can. J. Physiol. Pharmacol.* **70**, S64-S72
27. Putney, J.W., Jr. (1990) Capacitative Ca^{2+} entry revisited. *Cell Calcium* **11**, 611-624
28. Ganitkevich, V.Ya. and Isenberg, G. (1993) Membrane potential modulates inositol 1,4,5-trisphosphate-mediated Ca^{2+} transients in guinea-pig coronary myocytes. *J. Physiol.* **470**, 35-44
29. Muallem, S., Pandol, S.J., and Beeker, T.G. (1989) Hormone-evoked calcium release from intracellular stores is a quantal process. *J. Biol. Chem.* **264**, 205-212
30. Wakui, M., Potter, B.V.L., and Petersen, O.H. (1989) Pulsatile intracellular calcium release does not depend on fluctuations in inositol trisphosphate concentration. *Nature* **339**, 317-320